ELSEVIER

Chemical Engineering Journal 139 (2008) 562–574

Chemical Engineering Journal

www.elsevier.com/locate/cej

Flow analysis by pulsed ultrasonic velocimetry technique in Sulzer SMX static mixer

M. Hammoudi [a], J. Legrand [b,*], E.K. Si-Ahmed [a], A. Salem [a]

[a] *USTHB, Faculté de Physique, Laboratoire de Mécanique des Fluides Théorique et Appliquée, BP 32, El Alia 16111, Bab Ezzouar, Alger, Algeria*
[b] *GEPEA, Université de Nantes, CNRS, UMR6144, CRTT-BP 406, 44602 Saint-Nazaire Cedex, France*

Received 28 April 2007; received in revised form 25 August 2007; accepted 5 September 2007

Abstract

An experimental investigation, by pulsed ultrasonic velocimetry technique has been conducted for flow analysis in Sulzer SMX static mixers in the transitional and turbulent flow regimes ($1030 < Re < 13{,}270$). Axial velocity profiles and turbulent intensity have been analyzed upstream, downstream and within the static mixer. Turbulence intensity is tracked as function of Reynolds number. In addition velocity and turbulent intensity profiles have been examined for eight circumferential probe positions downstream the SMX at $Z = 0.7D$. A circumferential dependence is observed and affects all the hydrodynamic parameters studied.

Keywords: Static mixer; SMX; Pulsed ultrasonic velocimetry

1. Introduction

The industrial use of static mixers is well established nowadays. The wide range of industrial applications covered by the latter such as continuous mixing, heat and mass transfer processes and chemical reactions attracted several authors. Some of the advantages of static mixers over dynamic mixers (stirred tanks) are that they have no moving parts, small space requirements, low or no maintenance cost and a short residence time. Static mixers can be used in different working conditions, i.e. laminar, transitional and turbulent flow regimes Godfrey [1] and Myers et al. [2]. The mixer elements are designed to split the flow into two or more streams, rotate them and then recombine them for a better mixing. The SMX-type is made of identical elements inserted in an housing tube of diameter D. The unit element, constituting the SMX, are positioned one after the other with a circumferential shift of 90°, ensures homogenisation of material properties. The understanding of fundamental process is always an open question in order to optimize the mixing [1,3]. Meanwhile, investigations on pressure drop [4–7], residence time distributions [8,6], experimental velocity profile downstream the static mixer with Laser Doppler Anemometry (LDA) [9], friction factor by polarographic techniques Morançais et al. [10] and Hirech et al. [11] are reported. A good review of flow through static mixer was done by Thakur et al. [3]. Recently Legrand et al. [12] analyzed the effect of a liquid dispersed phase on the wall flow structure in SMX by electrochemical method. To investigate laminar flow through static mixer, an alternative approach is the use of CFD codes. In the last decade several numerical study of flow through static mixers has been conducted [13–18].

Note that the scarcity of information about flow inside SMX static mixer is due to its complex structure, which makes non-intrusive investigation difficult. In the present work we attempt to use pulsed ultrasonic velocimetry technique for extracting the velocity and the turbulence intensity profiles in order to estimate the mixing performance of SMX mixer.

Knowledge of the velocity field and turbulence intensity is of interest for the investigation of convective phenomena and mixing process. One should note that few data regarding the SMX performance in the turbulent regime are available in the literature. In order to capture the main parameters intervening in such process fine investigation and measurements are required. Pulsed ultrasonic velocimetry (PUV), developed over the last 25 years, is a powerful technique for extracting velocity and turbulence intensity profiles in fluid engineering Takeda [19,20]. The choice of this experimental technique is based on its ability of measuring instantaneous velocity profile over a measuring

* Corresponding author. Tel.: +33 2 40 17 26 33; fax: +33 2 40 17 26 18.
E-mail address: Jack.Legrand@gepea.univ-nantes.fr (J. Legrand).

1385-8947/$ – see front matter © 2007 Elsevier B.V. All rights reserved.
doi:10.1016/j.cej.2007.09.016

Nomenclature

C_{eff}	speed of sound in the medium (m/s)
C_{gel}	speed of sound in gel (m/s)
C_p	speed of sound in wall (m/s)
d_p	estimated pore diameter (m)
D	diameter of control (m)
e	the size of blade (m)
E/E_{max}	relative echo modulus of ultrasonic beam
f	frequency of emission (Hz)
f_D	Doppler frequency (Hz)
H	element (bed) height (m)
l	represent the wall thickness (mm)
L	pore length (m)
Pi	circumferential probe position
Q	flow rate (m^3/s)
r	radial coordinate
$Re = U_b D\rho/\mu$	Reynolds number
$Re_p = U_p d_p \rho/\mu$	pore Reynolds number
$U_b = 4Q/\pi D^2$	bulk velocity (m/s)
U_P	$\tau(U_b/\varepsilon)$
V	axial component of velocity (mm/s)
x	x-coordinate (m)
y	y-coordinate (m)
z	z-coordinate (m)

Greek symbols

α	external angle (°)
ε	average porosity of the SMX = 0.9
θ	Doppler angle (°)
μ	dynamic viscosity (0.779×10^{-3} Pa s)
ρ	density (992) (kg/m^3)
$\tau = L/H$	tortuosity of the SMX = 1.46

line, of its applicability to opaque pipes as well as emulsion with large concentration, mud, liquid metals [21,22].

In the present work, the flow in vertical duct of diameter D, equipped with Sulzer SMX static mixers, is described by a Reynolds number, based on bulk velocity and pipe diameter, outside the SMX and ranging from 1030 to 13,270 ($490 < Re_p < 6320$). The conventional Reynolds number has been substituted, within the static mixer, by the pore Reynolds number, Re_p. The latter takes into account the complex geometric structure of the SMX static mixer. According to Morançais et al. [10], Re_p is defined by considering the static mixer as a porous medium and by using a capillary model in terms of pore diameter d_p and tortuosity, τ, of the SMX element, with $d_p = 15.15$ mm and $\tau = 1.46$ in the present study.

The measurement with pulsed ultrasonic velocimetry (PUV) method are performed upstream, within and downstream the static mixer, in order to globally analyze the effect of static mixer on flow structure. The turbulence intensity is analyzed in term of rate of rate of mixing with respect to axial positions and Reynolds number.

2. Experiments

2.1. Experimental set-up

The experimental set-up is constituted by a pipe with an inside diameter of 50 mm and an overall length of 14D. The pipe is made of two identical parts interconnected by the housing tube of four elements of static mixer, SMX 50 (see Fig. 1). The ultrasonic probe can be displaced along the pipe and is localized as Z1 before the SMX, Z2 after the latter and by Z0 within the forth elements of the mixer. It should be noted, the value used for the angle α is 84° within the SMX, whereas on both sides mixer the angle of attack (external angle) used is of 72° (see Fig. 3). The first choice is governed by the skeleton of the matrix constituting the SMX while the second choice, for α, corresponds to the optimal value adopted in the literature. The working fluid (water) properties are taken at $T = 30$ °C, with density $\rho = 992$ (kg/m^3) and dynamic viscosity $\mu = 0.779 \times 10^{-3}$ (Pa s). The Z reference (Fig. 1) is taken in the entry of the static mixer: Z1 = $-D$; Z0 = 3.5D; Z2 = 4.7D.

It is advisable to recall that the number of blades of width equal to $e = 6.25$ mm = 0.125D (Fig. 2) contained in the duct are eight, two consecutive blades form an angle of 90° at the centre of the tube. Eight circumferential probe positions Pi ($1 < i < 8$) are carried downstream the static mixer and are located at Z2 = 4.7D (Fig. 2).

2.2. Pulsed ultrasonic velocimetry technique (PUV)

The pulsed ultrasonic velocimetry (PUV) technique has been used to obtain velocity profiles outside and inside the Sulzer SMX (Fig. 1). Such experimental method (PUV) has been chosen because it is the only one method giving the possibility to obtain velocity profile inside the static mixer. Moreover, the determination of the velocity does not need any calibration, and the method can be extended to study emulsion and mud.

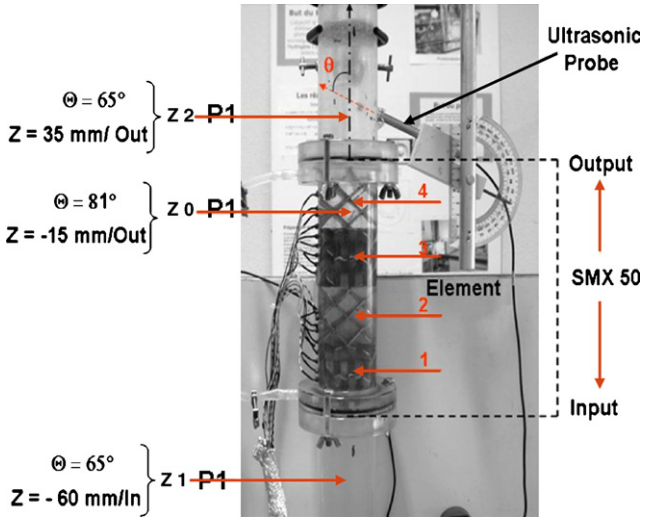

Fig. 1. Ultrasonic axial probe positions (Z1: upstream, Z2: downstream, and Z0: within the static mixer).

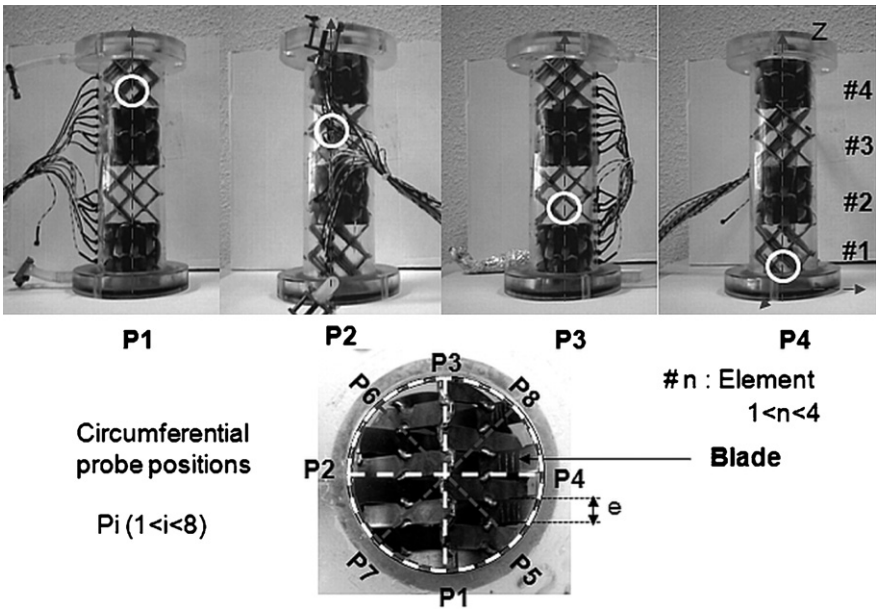

Fig. 2. Schema of axial motif and the circumferential ultrasonic probe position on duct: Pi ($1 < i < 8$) represents the circumferential ultrasonic probe positions.

The PUV method is based on the pulsed echo technique. A single transducer (TR30405 of Signal Processing) [23] with 4 MHz frequency emits the ultrasonic pulses beam and receives the echoes. All moving micro-particles suspended in the measured fluid are considered like sound tracer. They induce a frequency shift in the echo due to their movement. The velocity information is extracted by measuring these frequency shifts. The measurement of the delay between the burst emission and its reception gives the position of the scattering volume. The PUV apparatus (DOP 1000, Signal Processing S.A) [23] gives mean velocity, standard deviation, minimum and maximum velocity for each position using generally 512 emissions/profile. These data allow to obtain velocity and turbulence intensity profile. The velocity is calculated from the following expression:

$$V = \frac{C_{\text{eff}} f_{\text{D}}}{2 f \cos(\theta)} \tag{1}$$

In order to get accurate velocity profile the knowledge of the effective sound celerity C_{eff} in the medium and the attack angle θ of the ultrasound beam are of importance. f, f_{D} are, respectively, the frequencies of emission (4 MHz) and Doppler shift.

2.2.1. Parameters of measurements

The ultrasonic beam propagation is schematised in Fig. 3. The information required along the ultrasound shot is:

- C_{eff}: the effective sound velocity in fluid which is function of temperature, pressure and phase concentration.
- C_{gel}: the effective velocity in the interface; in our case a gel with $C_{\text{gel}} = 1103$ m/s.
- C_{p}: the effective velocity in the material used as tubing; here $C_{\text{p}} = 2820$ m/s (Altuglas).

All these parameters are used in the determination of the angles prevailing along the ultrasound beam course and expressed as follows:

$$\begin{cases} \dfrac{\cos(\beta)}{\cos(\alpha)} = \dfrac{C_{\text{P}}}{C_{\text{gel}}} \\ \dfrac{\cos(\vartheta)}{\cos(\beta)} = \dfrac{C_{\text{eff}}}{C_{\text{P}}} \end{cases} \Rightarrow \vartheta = \arccos\left(\frac{C_{\text{eff}}}{C_{\text{gel}}}\cos(\alpha)\right) \tag{2}$$

One should note that the evaluation of C_{eff} requires some care. As long as the tracer (particles) size is smaller than the ultrasound wavelength an effective homogeneous medium can be assumed.

For water, the sound velocity is given by Kinsler [24]:

$$C[\text{w}] = 1402.7 + 4.88T - 4.82 \times 10^{-2}T^2 + 1.35 \times 10^{-4}T^3 \tag{3}$$

at 30 °C, $C[\text{w}] = 1509.365 \approx 1509$ m/s.

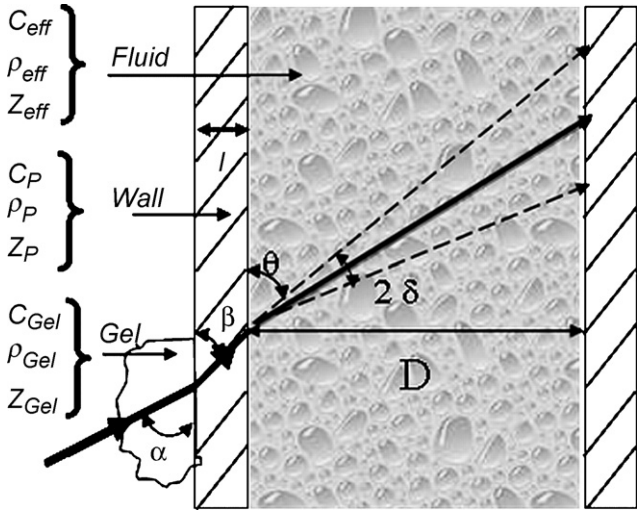

Fig. 3. Schematic of ultrasonic beam propagation.

2.2.2. Theoretical and experimental estimation of the angles

The velocity profile measurement is strongly dependent on θ, angle between the ultrasound beam and the main flow direction. Taking into account the fact that the method is non-intrusive, the angle is estimated from the external angle α and Eq. (2). There are various ways of determining θ. An accurate method consists in fixing the external angle α [21]. Unfortunately, such method has the disadvantage of having a fixed probe at the test section wall and thus cannot be displaced. However, the evaluation of θ becomes quite precise with the use of Eq. (2) and the medium sound velocity. For example Brito et al. [21] used three probes externally positioned at angles of 0°, 32° and 40°. Similarly, Eckert and Grebeth [25] have set a probe with an angle of 70°.

Another technique would be the insertion of the probe in a stagnant fluid having the same properties (sound celerity) of the flowing fluid: thus $\theta = \alpha$. The advantage of that configuration is that the probe can be displaced easily, but it has to be perfectly isolated and the stagnant fluid must be non-aggressive. Only water, at reasonable temperature, seems to be adequate.

Wada et al. [26] used such technique with three probes localised on the basis of an equilateral triangle and tilted by an angle of 45°, for an accurate estimation of flow rate. In the same way, Berni [27] showed an equivalent system where the probe, tilted by an angle of 65–70°, is immersed in a metal compartment surrounding the test section.

In the present work an experimental protocol has been elaborated based on the distal boundary position. As shown in Fig. 4 the distal wall can be easily identified since it displays a maximum of energy. In fact the position of the highest peak results from the interaction of the sound beam with the inside second wall which is fixed at $(D + l)$ where l represent the tube wall thickness. It happens that smaller peaks can be recorded, from each side of the main peak, due to sound beam divergence. Additionally, the distal wall is easily perceptible since the wall acoustical impedance Z_p is greater than the fluid one. It is recommended than the fluid should be at rest to avoid interferences of the acoustical impedance of scattering particles with the wall of the test section. Fig. 4 depicts the relative evolution of the modulus of the echo mode (E/E_{max}) according to the wall position. DOP 1000 gives a correspondence between θ and $(l + D)$. The basic approach can be summarized as follows: the inner wall position

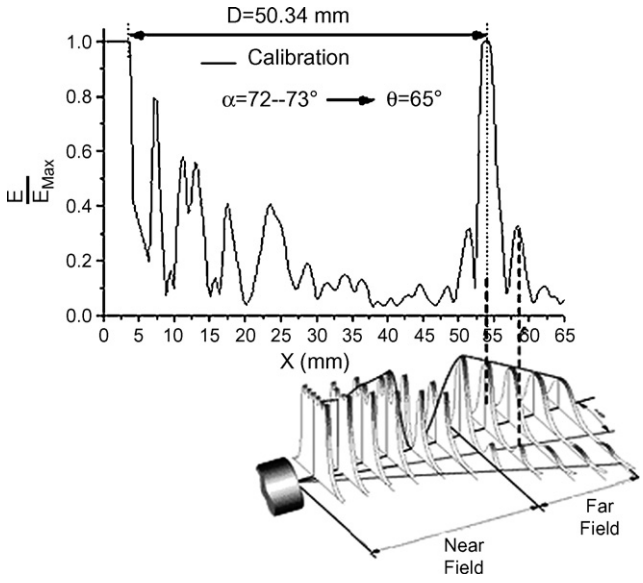

Fig. 4. Angle θ determination by the echo mode.

can be read, with a cursor available in the DOP 1000, and then related to θ. Any modification of the value of the angle θ will induce a peak displacement. The final value of θ is reached by varying step by step the angle until reaching the $(l + D)$ position for the main peak.

The validation of the PUV technique will be a posterior shown in Section 3.3.1 with the circumferential analysis of the axial velocity allowing the determination of the mean axial velocity.

3. Results and discussion

This experimental investigation covers data recordings for pore Reynolds number ranging from 490 to 6320. The Re_p number is based on pore diameter, d_p, and pore velocity U_p, in order to take into account the porous structure of SMX static mixer [10–12]. For the same Reynolds numbers, the profiles recorded upstream, inside the SMX (within the forth element constituting the static mixer) and downstream are reported. Outside the mixer, the Reynolds number used in the empty tube was based on pipe diameter D and bulk velocity U_b.

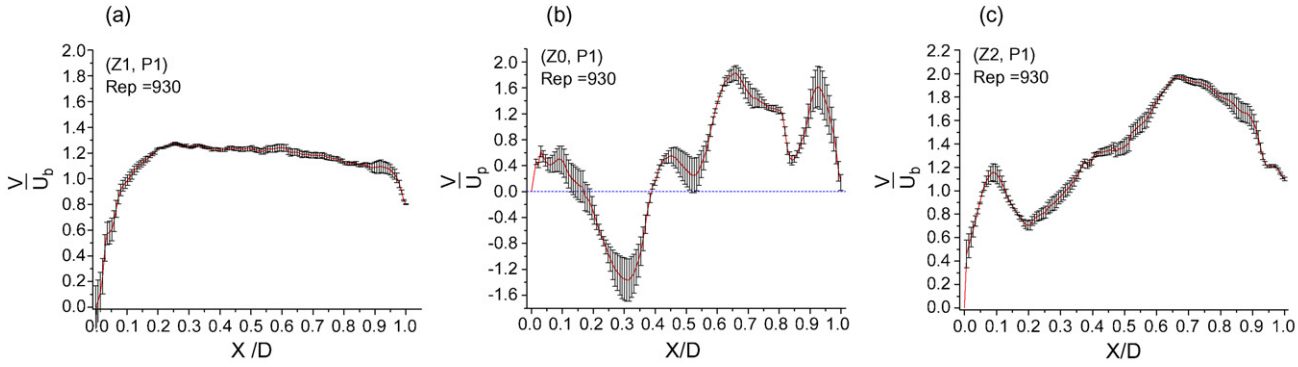

Fig. 5. Velocity profile for $Re = 1960$, $Re_p = 930$ at axial positions: (a) (Z1, P1), (b) (Z0, P1) and (c) (Z2, P1).

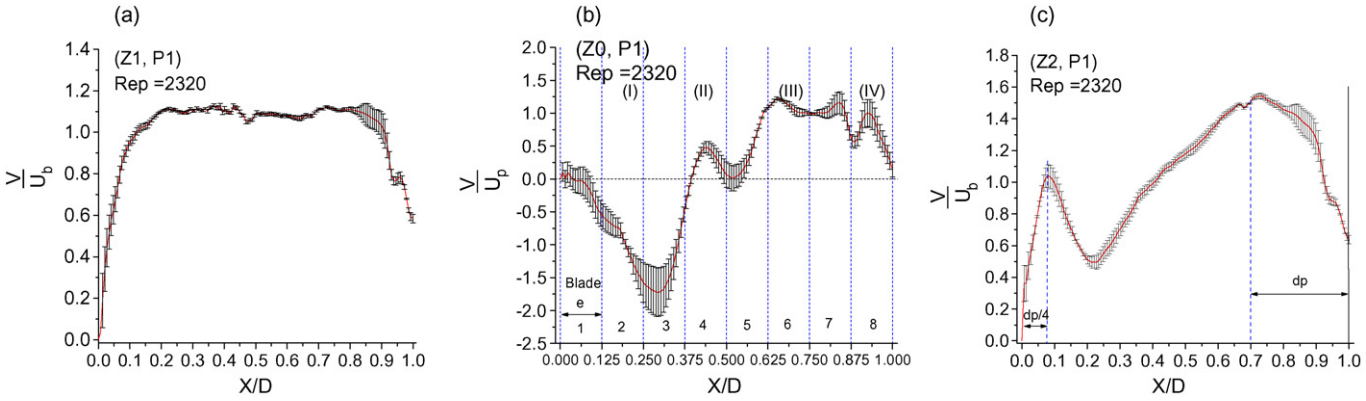

Fig. 6. Velocity profile for $Re = 4880$, $Re_p = 2320$ at axial positions: (a) (Z1, P1), (b) (Z0, P1) and (c) (Z2, P1).

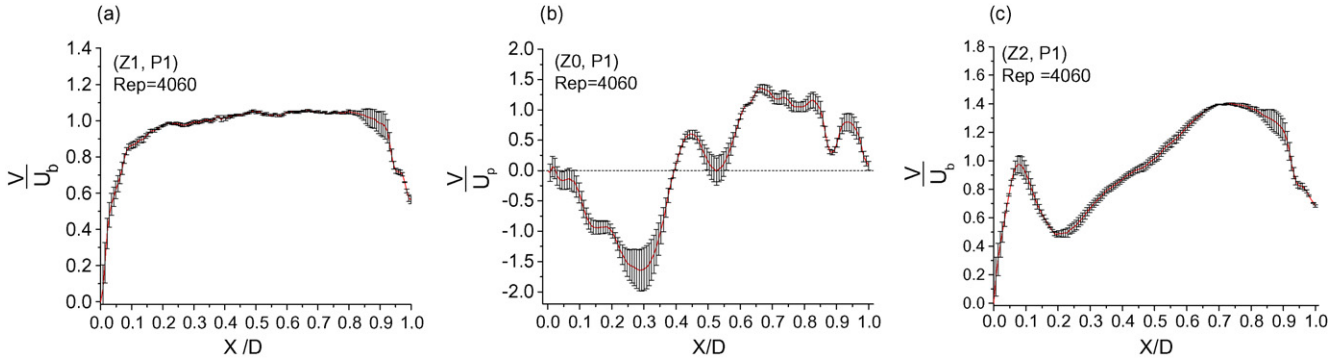

Fig. 7. Velocity profile for $Re = 8525$, $Re_p = 4060$ at axial positions: (a) (Z1, P1), (b) (Z0, P1) and (c) (Z2, P1).

3.1. Axial evolution of the velocity profiles

It should be noted that the velocity profile is not zero at the distal wall. This is due to an effect referred as "Ghost Flow" see [22,23,25], which is induced by the ultrasonic wave reflection on the distal wall perturbing then the recordings in the wall vicinity.

Flow upstream the SMX, Figs. 5a–8a reveal a flat velocity profile exhibiting then the turbulent nature of the flow. However, some quite fluctuations are recorded at $Re = 13{,}270$ ($Re_p = 6320$). This can be explained by the fact that the probe is positioned at only $1D$ from the static mixer (SMX) and therefore as the value of Re increases the influence of the obstacle is improved (see Fig. 8a).

Flow behaviour within the forth element of SMX is reproduced through Figs. 5–8b. Note that the $1D$ ultrasonic probe applied in PUV technique permit to extract both magnitude of the velocity component and flow direction. The velocity profiles are quasi identical with increasing Reynolds number. Negative values of velocity are recorded in the vicinity of the proximal wall and located between $0.05D$ and $0.4D$. Therefore in the proximal part of the measurement zone the presence of a recirculation zone of extent lower than $0.4D$ and a zone of fluid acceleration in the adjacent zone are revealed. The peak values are proportional to the flow rate. In the distal wall vicinity, it is observed the presence of a velocity peak with decreasing amplitude according to flow rate.

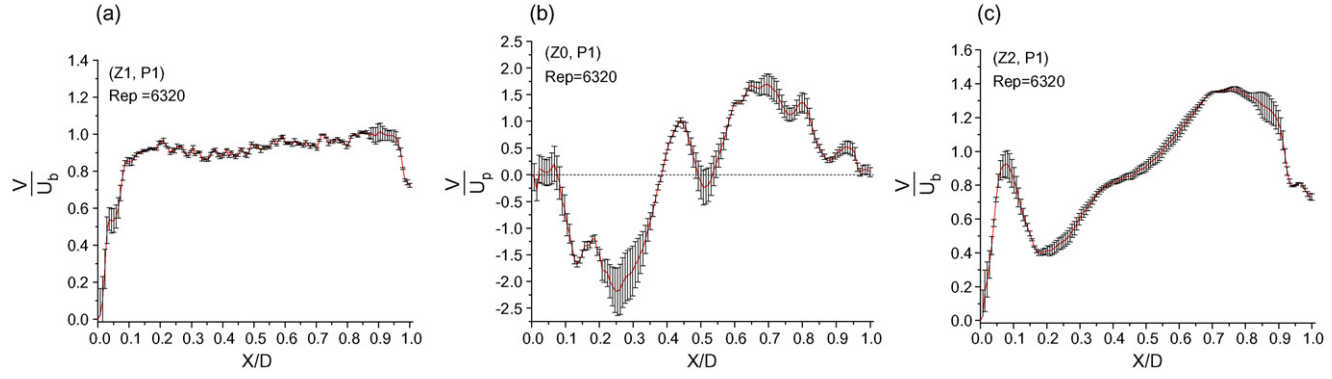

Fig. 8. Velocity profile for $Re = 13{,}270$, $Re_p = 6320$ at axial positions: (a) (Z1, P1), (b) (Z0, P1) and (c) (Z2, P1).

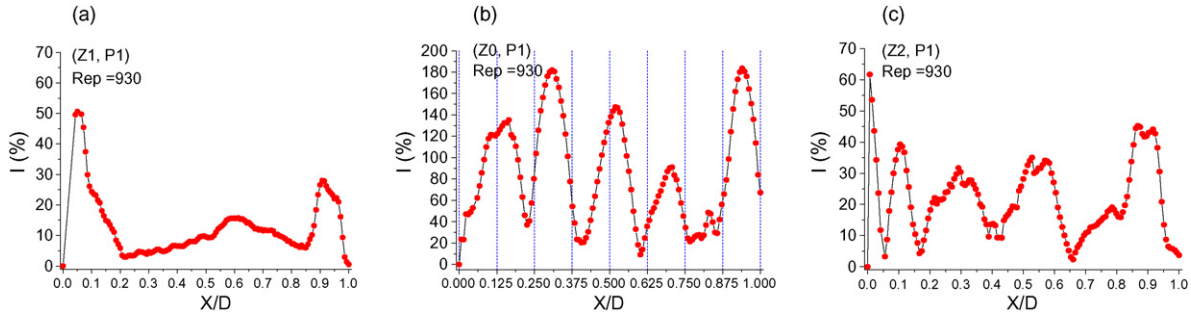

Fig. 9. Velocity profile for $Re = 1960$, $Re_p = 930$ at axial positions: (a) (Z1, P1), (b) (Z0, P1) and (c) (Z2, P1).

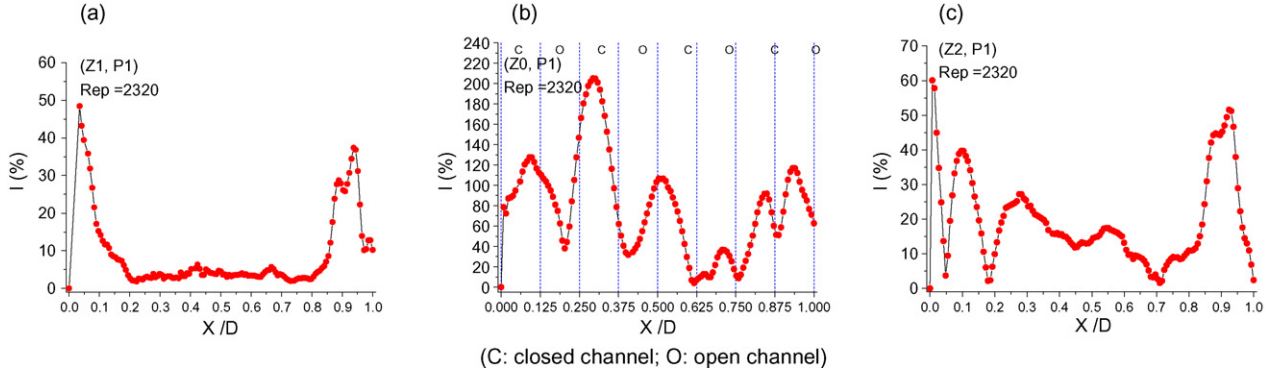

Fig. 10. Turbulence intensity profile for $Re = 4880$, $Re_p = 2320$ at axial positions: (a) (Z1, P1), (b) (Z0, P1) and (c) (Z2, P1).

Taking into account the interdependence between the fluid flow and the solid structure of the SMX, it is more convenient to refer the results to the radial position of the blade and their size $e = 0.125D$.

All the velocity profiles recorded in (Z0, P1) (see Figs. 1 and 2) highlight the presence of four distinct zones of flow (see Figs. 5b–8b):

- the first zone (I) includes the first three blades and has a radial distance of about $3e$: for Re_p between 930 and 6320, a negative peak is observed at $0.3D$, whose amplitude remains ranging between $1.2U_p$ and $1.9U_p$. Its position moves toward the wall with increasing Re. This observation suggests that the fluid flow direction is oriented from the core region mixer towards the proximal wall, corresponding to the arrangement of the blades of the SMX mixer at this measurement point;
- the second zone (II) corresponds to the fourth blade: a positive peak is present at the central part of the zone with an amplitude ranging between $0.6U_p$ and $0.8U_p$;
- the third zone (III) of $3e$ length includes five to seven blades: the zone is characterized by a somewhat flattened profile with an amplitude not exceeding $1.5U_p$;
- the last zone (IV) extends only on the eighth blade and presents a peak whose amplitude falls proportionally with Re, and passes from $1.6U_p$ to $0.2U_p$ for, respectively, $Re_p = 930$ and 6320.

All the profiles presented inside and downstream the SMX exhibit an asymmetrical behaviour to the non-circumferential symmetry of the SMX static mixer.

Downstream the SMX at (Z2, P1) (see Fig. 1) the velocity profile present two peaks, the first one is located at $d_p/4$ from the proximal wall while the second with higher amplitude is

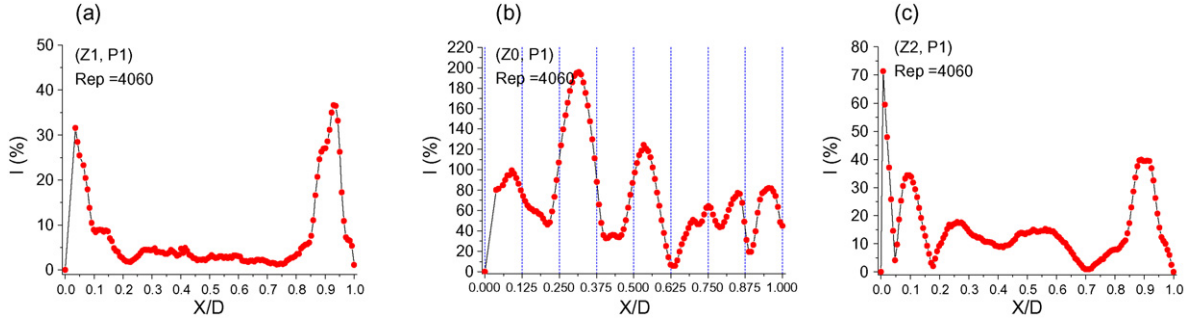

Fig. 11. Turbulence intensity profile for $Re = 8525$, $Re_p = 4060$ at axial positions: (a) (Z1, P1), (b) (Z0, P1) and (c) (Z2, P1).

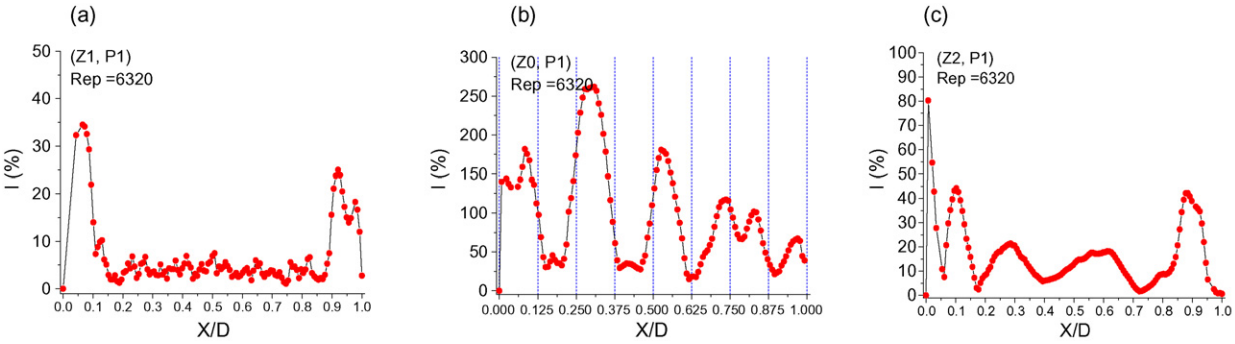

Fig. 12. Turbulence intensity profile for $Re = 13{,}270$, $Re_p = 6320$ at axial positions: (a) (Z1, P1), (b) (Z0, P1) and (c) (Z2, P1).

localized at d_p. The pore diameter d_p adopted in the present work, is about 15 mm and was determined by Morançais et al. [10].

Note that the behaviour of the velocity profile looks like the one met at the exit of a porous media, with the presence of a peak velocity in the wall area. Different works [28–30] locate the peak velocity at $d_p/4$ (see Fig. 7c).

The amplitude of the first peak is inversely proportional to Re and is equal to $1.1U_b$ and $0.90U_b$ for, respectively, $Re = 1960$ and 13,270, while the amplitude of the second one passes from $1.8U_b$ to $1.4U_b$. The study of the maximum value of the velocity shows a linear evolution, as function of the flow rates, on both sides of the mixer. However, a gap is noted downstream the SMX revealing then the mixer contribution by accelerating the fluid through the interstices available in its matrix.

3.2. Turbulence intensity

The instantaneous velocity is measured during a relatively short sampling time (149–462 ms) for each measuring point of the profile. It is possible to calculate the turbulent intensity along the probe axis based on the fluctuations of the instantaneous velocity measurements (Quadrio and Luchini [31]):

$$I\,(\%) = 100\frac{\sqrt{(u-\bar{u})^2}}{U} \tag{4}$$

where U is taken equal to pore velocity $U_p = \tau U_b/\varepsilon$ inside the static mixer and equal to the bulk velocity $U_b = 4Q/\pi D^2$ upstream and downstream the SMX.

The compared evolution of the turbulence intensity downstream, upstream and within the static mixer is examined. This information will allow estimating the index of mixing which is proportional of the turbulence intensity (Ting et al. [32] and Barrué et al. [33]).

Figs. 9–12 highlight the differences in turbulence intensity evolution for various probe axial positions (downstream, upstream and within the SMX). The increase of the flow rate does not modify the behaviour of the recorded curves. Upstream the mixer, Figs. 9a–13a reveal a flat profile of turbulence intensity in the core region with a decreasing evolution of its value according to Re from 13% to less than 5%. Meanwhile the maxima value of turbulence intensity is located in the vicinity of the walls and their amplitude decreases from 50% to 30%, respectively, for ($Re = 1960$–13,270) corresponding to ($Re_p = 930$–6320). In the wall region, the results are slightly higher than those encountered in the empty tube (20% and 30%) cited by Ref. [33].

Within the SMX at probe position (Z0, P1), the turbulence intensity profiles, (Figs. 9b–12b) reveals a periodical evolution, whose amplitude is on average 8.5 times greater than the one upstream. The increase in the flow rate does not modify the peaks location, but consequently modify their amplitude.

The minima of turbulence intensity are located downstream the blade two, four and between the fifth and sixth one. These positions are corresponding to the open channels (O) formed by the interlacing blades. Whereas the maxima values are positioned at the level of crossing blade (C) (Fig. 10b). The peak values of turbulence intensity have a no uniform evolution with respect to the first wall position. The increase of the flow rate generates a non-monotonous evolution of turbulence intensity peaks, while a decreasing evolution is observed upstream the SMX.

Downstream the SMX at probe position (Z2, P1), the velocity profile at the core region is characterized by a periodic evolution corresponding to the one observed inside the SMX (Figs. 9c–12c). However the maxima values decrease with respect to the Reynolds number. The values of the peak ampli-

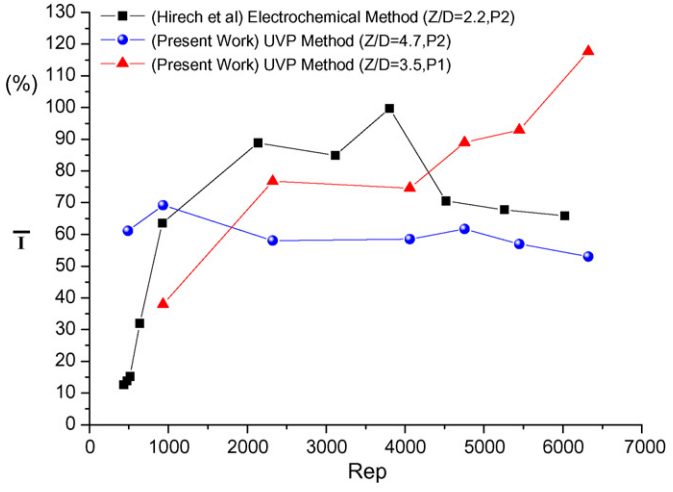

Fig. 13. Compared evolution of the average turbulence intensity at different measurement point according to two methods of investigation.

tude are generally 3 or 5 times greater than those encountered upstream the SMX. In the first wall region we can observe two peaks with decreasing amplitude according to their parietal positions. These two peaks are positioned in $d_p/2$ while the minima value between them is located at nearly $d_p/4$ corresponding to the maximum velocity. In the vicinity of the second wall the peak amplitude is not affected by the flow rate and remains constant at about 40%.

The average turbulence intensity within the SMX varies from 62% to 94% according to the flow rate whereas downstream it does not exceed 21.5%. However the curves show that the intensity of turbulence downstream the SMX is on average 1.5–2 times more important than upstream. The average turbulence intensity within the mixer is 6–11 times more significant than observed upstream the mixer (Figs. 9–12). The increasing of the flow rate produces a reduction of the average value of the turbulence intensity on both sides of the SMX. The increase of the flow rate differently influences I_{max} according to the axial position considered. Upstream SMX (Z1, P1), I_{max} decreases from 50% to 35% with increase of Re. Downstream the SMX (Z2, P1) I_{max} linearly increases from 60% to 80%, these values are of the same order of amplitude than the ones giving by Ref. [33]. These authors studied and compared the circumferential turbulence intensity evolution of flow through SMI, KMA and Oxynator® static mixers with a gas injection. The investigation by LDA technique reveals a circumferential dependence of the turbulence intensity. The maxima values of turbulent intensity are in the range of 40–130% for the Oxynator®, $I_{ave} = 60\%$ for the KMA and between 30% and 150% for certain circumferential position of the SMI static mixer.

Within the SMX (Z0, P1) I_{max} increases in a non-monotonous way and goes from 180% to 260%. It should be observed that these values are in conformity with the results presented in literature [33].

The objective of this paragraph is to compare the results obtained using PUV technique and those obtained by an electrochemical method [11], for the same experimental set-up. The electrochemical method allows determining the local near-wall flow characteristics such as the wall shear stress or the wall-turbulence characteristics Hanratty and Campbell [34]. While the PVU technique estimate the turbulence intensity profile with the fluctuation term of velocity. In the wall region the velocity gradient fluctuation rate is comparable to the velocity fluctuation intensity.

Each SMX element has four facets (see Fig. 2) with symmetry of rotation equal to 180°, P1 and P3 have the same motif (design), while P2 and P4 have another one.

As shown in Fig. 2, the axial positions surrounded by a circle are identical and expose the same geometry to the fluid flow. The axial positions marked and located in elements #3 and #4 correspond, respectively, to ($Z = 2.2D$, P2) and ($Z0 = 3.5D$, P1), which allow to compare the evolution of the hydrodynamic parameters collected in these two points. The first position ($Z = 2.2D$, P2) corresponds to measurement obtained by the electrochemical method [11], whereas in the second position ($Z0 = 3.5D$, P1), measurements were made by VUP technique. Fig. 2 shows the helicoidal axial displacement of the basic motif constituting the static mixer formed by the four elements positioned one after the other with a circumferential shift of 90°.

Fig. 13 depicts the compared evolution of the turbulence intensity according to the flow rate as well as to axial and circumferential positions. The average turbulence intensity $\bar{I}$ obtained at positions ($Z/D = 2.2$, P2) and ($Z/D = 3.5$, P1), respectively, at the entrance of the third and forth SMX element reveal a similarity evolution up to Re_p 3500 in transitional flow regimes. An increase of the average turbulence intensity according to the flow rate is observed with both methods. Beyond $Re_p = 4000$ in turbulent regime, a difference in evolution is observed between the two positions; the electrochemical probe located at ($Z/D = 2.2$, P2) shows a decreasing progression with Re_p while the measurement provided by UVP method reveal an increasing evolution according to the flow rate. The average turbulence intensity values derived from UVP method and located at the exit of the SMX static mixer show a nearest constant evolution with Re_p.

In general the differences observed between the values extracted from different positions can be explained by the axial and circumferential dependencies of $\bar{I}$ measurements and by the nature of the method used. In fact, the electrochemical method allows a local estimation of $\bar{I}$, while the estimation of this parameter with PUV method is obtained by averaging the value of turbulence intensity in the near-wall region.

3.3. Circumferential evolution of the flow characteristics

The complexity of the structure of SMX mixer does not allow a circumferential study inside the mixer. A circumferential study of the flow was carried out at $0.7D$ downstream the SMX mixer. Eight circumferential probe positions Pi ($1 < i < 8$) have been necessary in order to describe the flow distribution as well as possible and to try to present a 3D representation of mean velocity and turbulence intensity. The eight circumferential probe positions, referred hereafter by Pi ($1 < i < 8$), are separated by 45° (Fig. 2).

3.3.1. Velocity profile

The circumferential velocity distributions, at $Z = 4.7D$ are depicted in Figs. 14 and 15. They highlight an asymmetric character of the flow behaviour downstream the SMX static mixer.

The behaviour of the profile is related with the complex geometry of the blades and their circumferential orientation (Fig. 16a–d).

The directions (P1, P3) and (P7, P8) reveal a peak above the first and the last blade while the plans formed by (P2, P4) and (P5, P6) shows a fading parabolic evolution due to the inclination of the blade. Note that in the direction (P7, P8) at $r = 0$, the difference between the velocity coming from P7 and P8 beams (Fig. 16c). The difference is inherent to the PUV technique which extracts the velocity profile a long an inclined beam. This difference allows to estimate at $r = 0$ the maximum angle between the velocity vector and the axial direction of flow which is about 17° while Visser et al. [35] exhibit the maximum angle

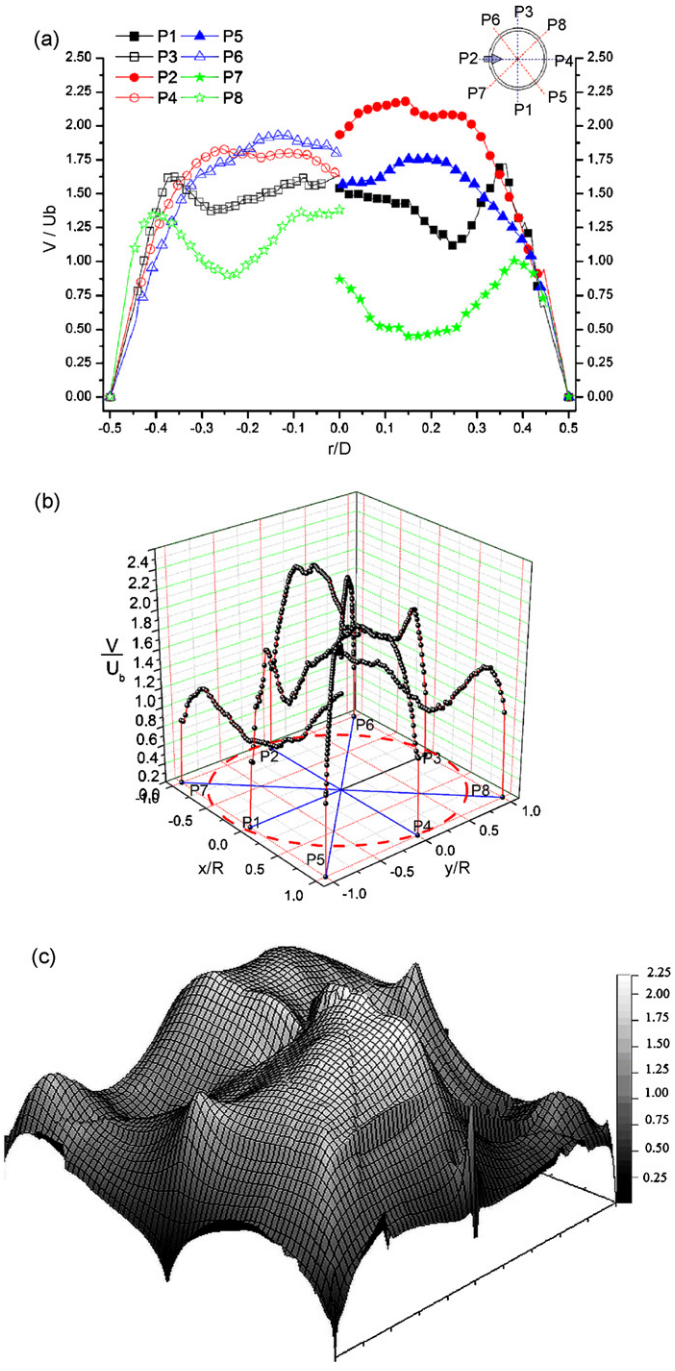

Fig. 14. Flow mapping at $Re = 1030$. Different representations of the velocity profile. (a) 2D representation of velocity profile according to circumferential positions. (b) Three-dimensional representation of profile velocity. (c) Volumetric estimation of the flow according to the eight profiles data.

between the velocity vector and flow axial direction about 19° in a three-dimensional numerical simulation of laminar flow in duct with a square cross-section containing two, four and eight blades.

For all the flow rates studied, the maximum velocity is located at circumferential position P2 and $0.3D$ from the wall while the minima value is at $0.35D$ and coming from P7. The circumferential position P7 show a negative velocity for $Re > 4800$, revealing a recirculation zone.

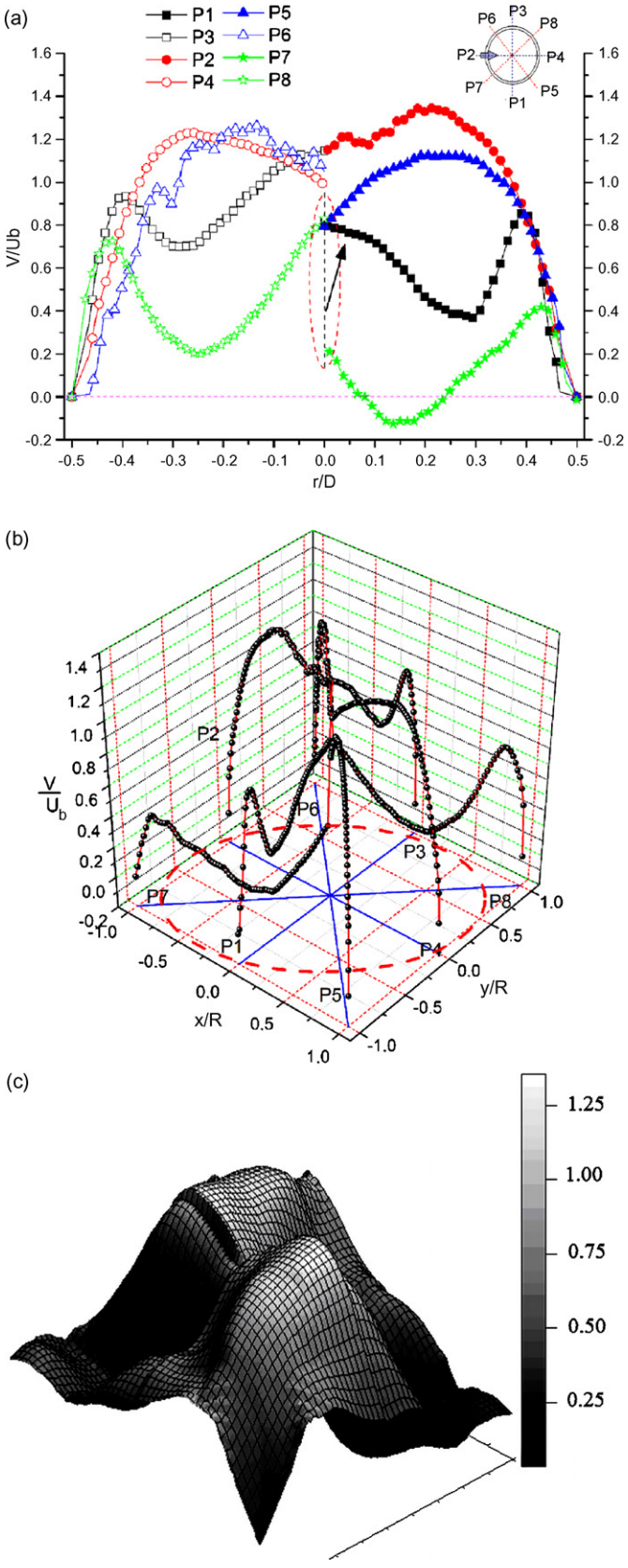

Fig. 15. Flow mapping at $Re = 13{,}270$. Different representations of the velocity profile. (a) 2D representation of velocity profile according to circumferential positions. (b) Three-dimensional representation of profile velocity. (c) Volumetric estimation of the flow according to the eight profiles data.

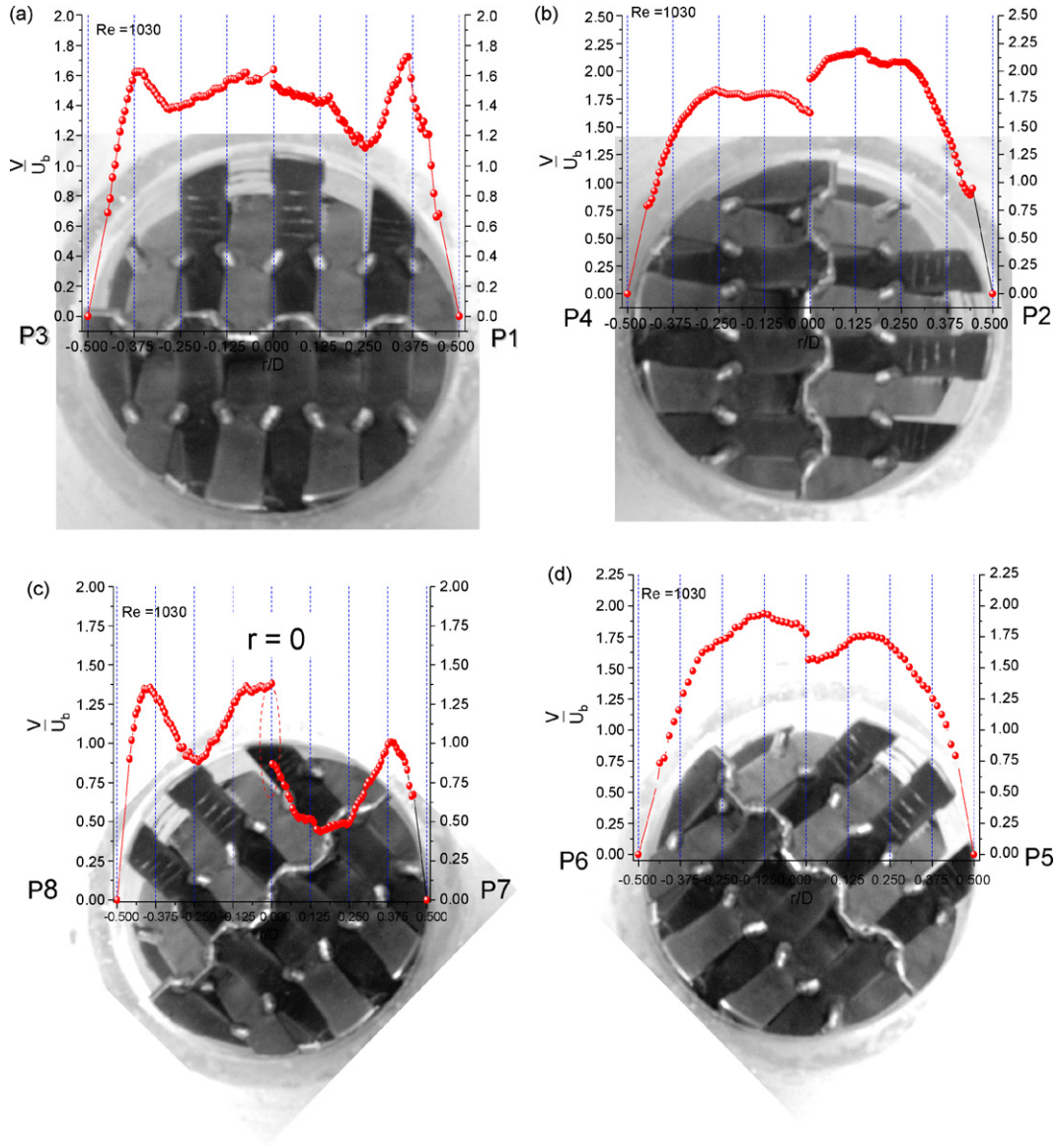

Fig. 16. Evolution of velocity profile according to the measured line, localized at $Z = 35$ mm downstream the SMX static mixer for $Re = 1030$: (a) (P1, P3); (b) (P2, P4); (c) (P7, P8); (d) (P5, P6).

The increasing of the flow rate from ($Re = 1030$–13,270) does not change the behaviour of the profile but modify the amplitude of peaks values. The maximum value of velocity decrease from $2.2U_b$ to $1.35U_b$ at the P2 position while the minima value passes from 0.4 to $-0.125U_b$ at P7 position.

The results presented are compared to those from various static mixers (Oxynator, KMA, and SMI) performed by Ref. [33]. Some similarities are observed: on one hand, the circumferential dependence of hydrodynamic parameters encountered within and downstream the static mixers of type (SMX and Oxynator, and SMI [33]) and, on the other hand the order of magnitude of the velocity fluctuations (see Fig. 17). At Reynolds number equal to 82,000, a circumferential dependency of the axial velocity V is observed for the Oxynator and SMI static mixers, respectively, $-0.9U_b < V < 1.7U_b$, for the first and $0.5U_b < V < 2U_b$ for the second, while this dependency is smaller in the KMA static mixer, where V is in the range of $[1.2U_b, 1.8U_b]$.

In addition the velocity profiles of the eight circumferential probe positions allow to estimate a three-dimensional plot of axial velocity. For this purpose a rather fine grid based on Kriging method (Abramowitz and Stegun [36], Cressie [37]) with an identical grid mesh $\Delta x = \Delta y = 0.375$ mm is used. Kriging method produces maps from irregularly spaced data (Figs. 14c–15c). Once the profile 3D obtained, it is easy to calculate the volume by using an extended Simpson's 3/8 rule of surface integration.

The comparison (Fig. 18) of the flow rate values obtained from PUV measurement with the ones given by the flow meter from $Re = 1030$ to 13,270 allows to validate the experimental PUV method. A good agreement between the two methods is obtained with relative error of about 7.5%.

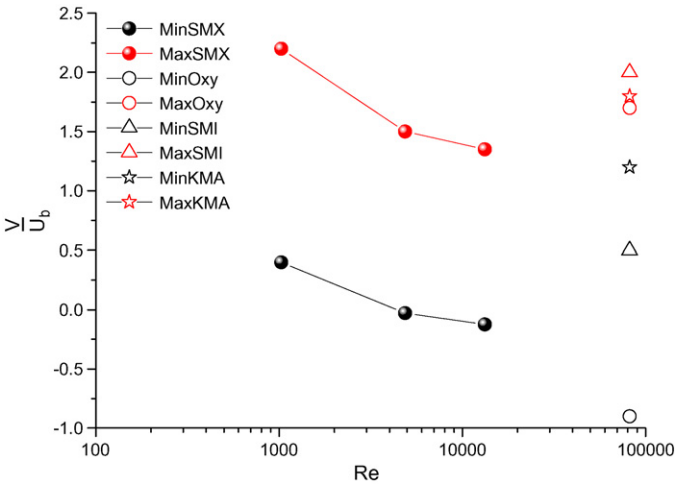

Fig. 17. Compared evolution of the maximum values of velocity profile coming from Oxynator, SMI, KMA (Barrué et al., 2001) and SMX (present work).

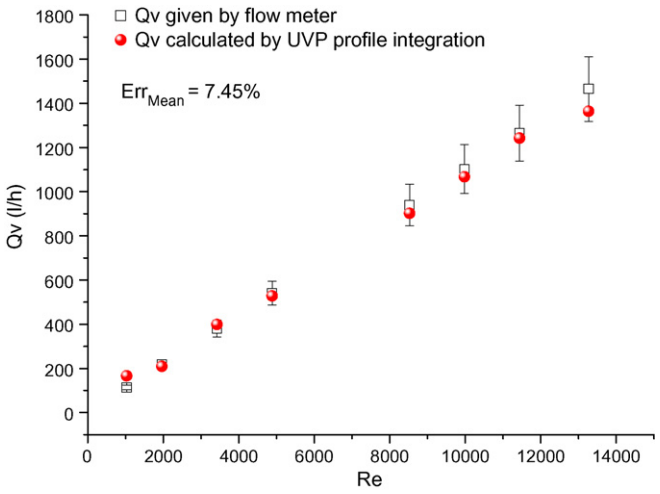

Fig. 18. Compared evolution of two methods estimation of the flow rate.

3.3.2. Turbulence intensity

Fig. 19 depict a comparative turbulence intensity profile according to the circumferential positions. The angular dependency was clearly shown and the geometry of the SMX significantly influences the turbulence intensity profile.

Fig. 20a–d, allow to relate the peak locations and the blade positions.

As previously observed for the velocity profiles, we distinguish the existence of two types of turbulence intensity profiles. The first group (P1, P3, P7 and P8) presents several peaks located at the top of the intersections of the blades. The minima are inserted between the peaks and are located above the passage areas between the blades intersections. One notes a periodic character in the case of (P7, P8) orientation according to a diagonal direction compared to the orientation of the blades. The position and the number of the minima are connected to the areas of passages (open channels) according to this direction. The second group (P2, P4, P5 and P6) presents a parietal peak corresponding to the closed area of length of about 0.175*D* (see Fig. 20b). The extent of this area is slightly more important in the case of a direction (P5, P6) because of its diagonal orientation. The central area presents a peak of less amplitude two at three times lower.

3.3.3. Practical implications of the work

The flow analysis reported in the work is really the first experimental study to characterize the flow structure inside a static mixer. The flow is rather heterogeneous inside the static mixer with a large recirculation zone near the proximal wall, which can explain a part of the axial dispersion observed for flow through static mixer. The high turbulence intensities observed inside the static mixer show that SMX is a very good turbulence promoter to improve heat, mass and mixing phenomena, even for low Reynolds numbers. It is also noticeable that the turbulence intensity is very rapidly damped at the outlet of the static mixer. The circumferential evolution of the hydrodynamic parameters has also to taken into account according to the application of the static mixer. For example, it is necessary to have a sufficient number of elements in order to have a rather uniform treatment. The minimal length seems to be four elements for transitional and turbulent flow regimes, as already reported by Ludwig [38] for some processes like waste water neutraliza-

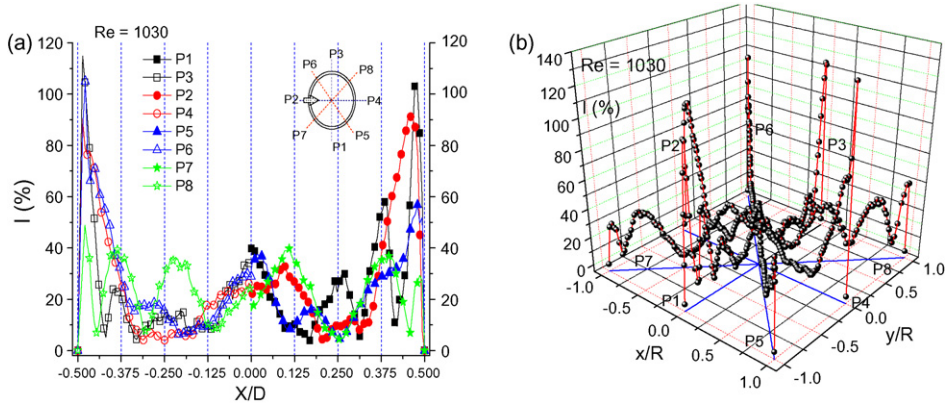

Fig. 19. Turbulence intensity profiles according to circumferential probe positions localized at $Z = 0.7D$ downstream the SMX, for $Re = 1030$: (a) 2D profiles comparison and (b) 3D representation.

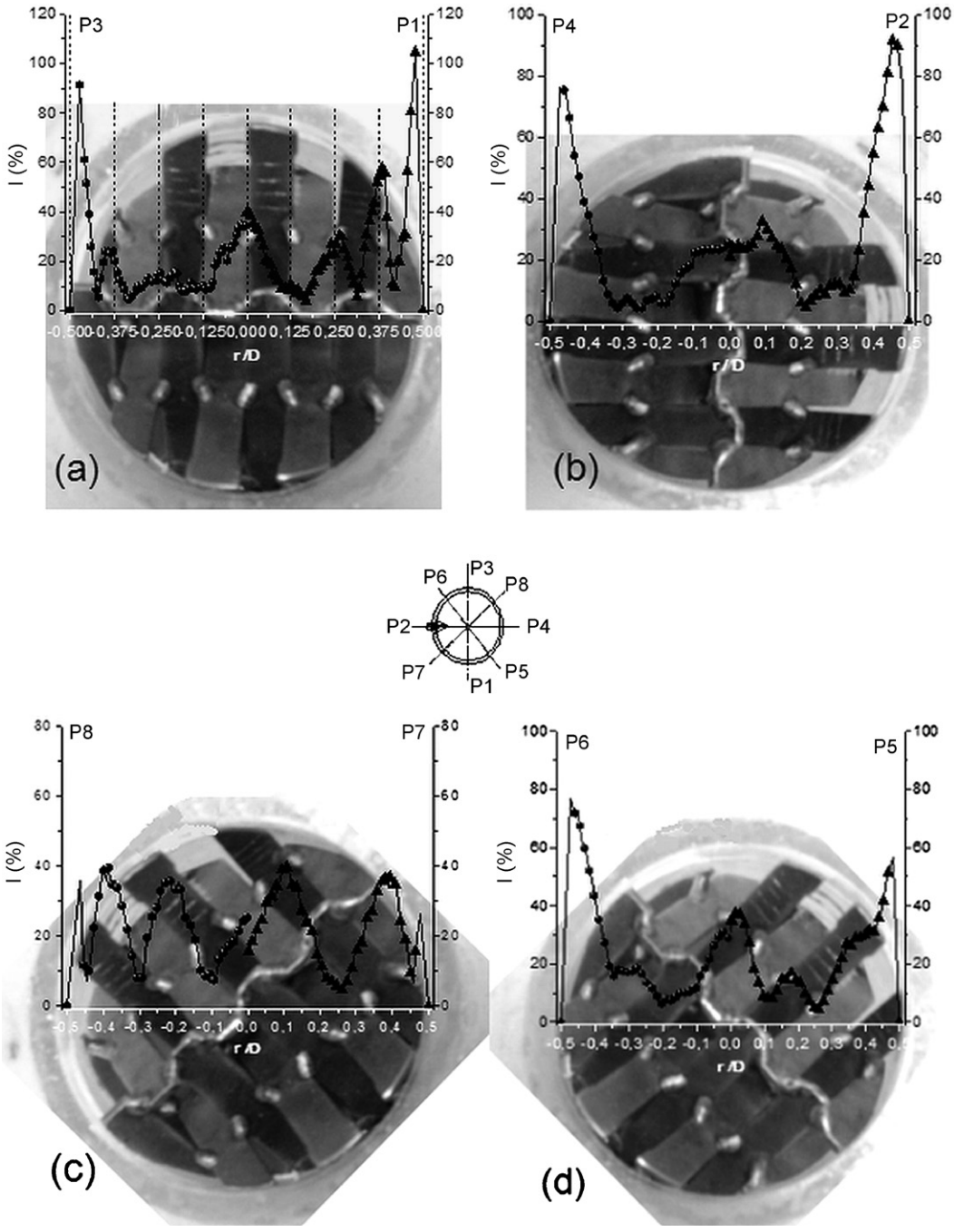

Fig. 20. Evolution of turbulent intensity profile according to the measure line, located at $Z = 35$ mm downstream the SMX static mixer for $Re = 1030$: (a) (P1, P3); (b) (P2, P4); (c) (P7, P8); (d) (P5, P6).

tion or liquid–liquid blending to obtain homogenous product. On the other hand, the pulsed ultrasonic method, which has been validated in this study, can be further used to investigate the formation of gas–liquid and liquid–liquid two-phase flow. One objective would be to analyze the break-up phenomena occurring in theses static mixers.

Moreover, the reported measurements will definitely serve as reference results, both local and averaged hydrodynamic data, for numerical simulations in a rather large (transitional and turbulent flow) flow range.

4. Concluding remarks

The velocity profile and turbulence intensity has been investigated, by pulsed ultrasonic velocimetry, at three axial probes positions upstream, within and downstream the SMX. Upstream SMX, flat velocity profiles are noted while substantial modifications of these profiles are observed, within the mixer. Profiles are divided into two distinct areas: proximal and distal areas, respectively. The first area is a recirculation zone where velocities are negative with a maximum at $0.3D$ whose intensity is propor-

tional to the flow rate. The second zone is a zone with multiple velocity peaks whose intensity is proportional to the flow rate. In general, the velocity profiles have a non-monotonous form leading to a periodical function with respect to the wall position. Downstream the static mixer, the velocity profile presents a peak in the vicinity of each wall, the distal peak is greater than the proximal. The increase of flow rate does not modify the shape of the curves, but only the amplitude of the peaks. The study of the turbulence intensity highlighted the local character of mixing. Upstream of the mixer the average turbulence intensity decrease with the flow rate and is in conformity with the literature relating to empty duct whereas downstream the SMX it is nearly two times greater but decrease with an increasing of the flow rate. The most significant variations of the turbulence intensity are observed within the SMX. The circumferential study downstream the static mixer permits to identify two categories of velocity profiles. The first groups (P1, P3, P7 and P8) exhibit a peak velocity at the wall vicinity while the second group formed by (P2, P4, P5 and P6) reveal a fading parabolic evolution. The increase of flow rate does not modify the shape of the curves. The evolution of velocity profile and turbulence intensity is closely related to the structure of the SMX static mixers.

Acknowledgement

The authors wish to thank SONATRACH for the support provided on conducting this study.

References

[1] J.C. Godfrey, Static mixers, in: N. Harnby, M.F. Edwards, A.W. Nienow (Eds.), Mixing in the Process Industries, 2nd ed., Butterworth-Heinemann, Oxford, 1992, pp. 225–249.
[2] K.J. Myers, A. Bakker, D. Ryan, Static mixer fundamentals and applications, Chem. Eng. Proc. 93 (1997) 28–38.
[3] R.K. Thakur, C. Viala, K.D.P. Nigam, E.B. Nauman, G. Djelveh, Static mixers in the process industries—a review, Trans. Inst. Chem. Eng. 81 (2003) 787–826.
[4] W.L. Wilkinson, M.J. Cliff, An investigation into the performance of static in-line mixer, in: Proceedings of the Second European Conference on Mixing (BHRA), 1977, pp. A2–A15.
[5] N.F. Shah, D.D. Kale, Pressure drop for laminar flow of non-Newtonian fluids in static mixers, Chem. Eng. Sci. 46 (1991) 2159–2161.
[6] H.Z. Li, C. Fasol, L. Choplin, Residance time distribution of rheologically complex fluid passing through a Sulzer SMX static mixer, Chem. Eng. Commun. 165 (1998) 1–15.
[7] S. Liu, A.N. Hrymak, P.E. Wood, Laminar mixing of shear thinning fluids in a SMX static mixer, Chem. Eng. Sci. 61 (2005) 1753–1759.
[8] E.B. Nauman, On residence time and trajectory calculations in motionless mixers, Chem. Eng. J. (1991) 141–148.
[9] A. Karoui, F. Hakenholz, N. Lesauze, J. Costes, J. Bertrand, Determination of mixing performance of Sulzer SMV static mixers by fluorescence, Can. J. Chem. 70 (1998) 522–526.
[10] P. Morançais, K. Hirech, G. Carnelle, J. Legrand, Investigation of friction factor in static mixers, Chem. Eng. Commun. 171 (1999) 77–93.
[11] K. Hirech, A. Arhaliass, J. Legrand, Experimental investigation of flow regimes in an SMX Sulzer static mixer, Ind. Eng. Chem. Res. 42 (2003) 1478–1484.
[12] J. Legrand, K. Hirech, A. Arhaliass, Effect of liquid dispersed phase on the wall flow structure in static mixer, Int. J. Multiphase Flow 32 (2006) 593–605.
[13] Th. Avalosse, M.J. Crochet, Finite element simulation of mixing. 2. Three dimentional flow through a Kenics mixer, AIChE J. 43 (3) (1997) 588–597.
[14] L. Fradette, H.Z. Li, L. Chauplin, P.A. Tanguy, 3D finite element simulation of fluid through a SMX static mixer, Comput. Chem. Eng. 22 (1998) 759–761.
[15] O. Byrde, M.L. Sawley, Parallel computation of flow in an in-line static mixer, in: J.-A. Désidéri, et al. (Eds.), Proceedings of the Third ECCOMAS Computational Fluid Dynamics Conference, Wiley, New York, 1996, pp. 802–807.
[16] D. Rauline, P.A. Tanguy, J.M. Le Blevec, J. Bousquet, Numerical investigation of the performance of several static mixers, Can. J. Chem. Eng. 76 (1998) 527–535.
[17] D. Rauline, J.M. Le Blevec, J. Bousquet, P.A. Tanguy, A comparative assessment of the performance of the Kenics an SMX static mixers, Trans. Inst. Chem. Eng. 78A (2000) 389–395.
[18] E. Fourcade, R. Wadley, H.C.J. Hoefsloot, A. Green, P. Iedema, CFD calculation of laminar striation thinning in static mixer reactors, Chem. Eng. Sci. 56 (2001) 6729–6741.
[19] Y. Takeda, Development of an ultrasound velocity profile monitor, Nucl. Eng. Des. 126 (1991) 277–284.
[20] Y. Takeda, Velocity profile measurement by ultrasonic Doppler method, Exp. Therm. Fluid Sci. 10 (1995) 444–453.
[21] D. Brito, H.C. Nataf, P. Cardin, J. Aubert, J.P. Masson, Ultrasonic Doppler velocimetry in liquid gallium, Exp. Fluids 31 (2001) 353–363.
[22] T. Wang, J. Wang, F. Ren, Y. Jin, Application of Doppler ultrasound velocimetry in multiphase flow, Chem. Eng. J. 92 (2003) 111–122.
[23] Signal Processing S.A., Technical information and application notes, http://www.signal-processing.com, 2002.
[24] L. Kinsler, Fundamentals of Acoustics, 2nd ed., John Wiley and Sons, Inc., 1962.
[25] S. Eckert, G. Gerbeth, Velocity measurements in liquid sodium by means of ultrasound Doppler velocimetry, Exp. Fluids 32 (2002) 542–546.
[26] S. Wada, H. Kikura, M. Aritomi, M. Mori, Y. Takeda, Development of pulse ultrasonic Doppler method for flow rate measurement in power plant multilines flow rate measurement on metal pipe, J. Nucl. Sci. Technol. 41 (2004) 339–346.
[27] A. Berni, Unsteady velocity profiles and energy dissipation in turbulent pipe flow, PhD Thesis, University of Perugia Italia, 2005.
[28] B.C. Chandrasekhara, D. Vortmeyer, Flow model for velocity distribution in fixed porous beds under isothermal conditions, Warme Stoffubertrag. 12 (1979) 105–111.
[29] D. Vortmeyer, J. Schuster, Evaluation of steady flow profiles in rectangular and circular pecked beds by a variational method, Chem. Eng. Sci. 36 (1983) 1691–1699.
[30] N. Manjhi, N. Verma, K. Salem, D. Mewes, Simulation of 3D velocity and concentration profiles in a packed bed adsorber by lattice Boltzmann methods, Chem. Eng. Sci. 61 (2006) 7754–7765.
[31] M. Quadrio, P. Luchini, Direct numerical simulation of the turbulent flow in a pipe with annular cross section, Eur. J. Mech. B: Fluids 21 (2002) 413–427.
[32] W. Ting, S. Chintalapati, R.S. Bunker, C. Pang Lee, Jet mixing in a slot, Exp. Therm. Fluid Sci. 22 (2000) 1–17.
[33] H. Barrué, A. Karoui, N. Le Sauze, J. Costes, F. Illy, Comparison of aerodynamics and mixing mechanisms of three mixers: Oxynator™ gas–gas mixer, KMA and SMI static mixers, Chem. Eng. J. 84 (2001) 343–354.
[34] T.J. Hanratty, J.A. Campbell, Measurement of wall shear stress, in: J. Goldstein (Ed.), Fluid Mechanics Measurement, Hemisphere Publishing Corporation, Washington, 1983, pp. 559–615.
[35] J.E. Visser, P.F. Rozendal, H.W. Hoogstraten, A.A.C.M. Beenackers, Three-dimensional numerical simulation of flow and heat transfer in the Sulzer SMX static mixer, Chem. Eng. Sci. 54 (1999) 2491–2500.
[36] M. Abramowitz, I. Stegun, Handbook of Mathematical Functions, Dover Publications, New York, 1972.
[37] N.A.C. Cressie, Statistics for Spatial Data, John Wiley and Sons, Inc., New York, 1991.
[38] E.E. Ludwig, Applied process design for chemical and petrochemical plants, vol. 1, 3rd ed., Butterworth-Heinemann, 1999, p. 338.